Lo MM. 5104
ROMA

Nota Interna n. 304
22 gennaio 1971

Istituto di Fisica "G.Marconi"
Università di Roma
I.N.F.N. - Sezione di Roma

I.Bruner, U.Dore, P.Guidoni, I.Laakso, G.Martellotti, G.Marini, F.Massa, G.Piredda, P.Pistilli:

"PROJECT OF A Λ° MISSING MASS SPECTROMETER TO STUDY THE REACTION $\pi^{-} + p \longrightarrow \Lambda^{\circ} +$ NEUTRALS"

PROJECT OF A Λ° MISSING MASS SPECTROMETER TO STUDY THE REACTION $\pi^- + p \longrightarrow \Lambda^\circ$ + NEUTRALS

I.Bruner, U.Dore, P.Guidoni, I.Laakso, G.Martellotti, G.Marini,
F.Massa (*), G.Piredda, P.Pistilli
Istituto di Fisica dell'Università - Roma
Istituto Nazionale di Fisica Nucleare - Sezione di Roma

Abstract

We describe a counter-spark chambers apparatus designed to investigate the neutral missing-mass (M°) spectrum in the reaction $\pi^- + p \rightarrow \Lambda^\circ + X^\circ$, via the detection and measurement of the Λ°'s produced with small 4-momentum transfer ($\Delta^2_{p\rightarrow\Lambda^\circ} < 1\ (GeV/c)^2$). The physical interest in the exploration of the M° spectrum below 1.8 GeV/c^2, at incident π^- momenta between ~ 5 and 10 GeV/c, is briefly outlined. Estimates for the foreseen X° mass resolution, and the expected counting rates are also given.

(*) Present address - Istituto di Fisica Superiore, University of Naples, Naples, Italy.

I. - Introduction

This is a description of a " Λ° missing mass spectrometer", i.e. a counter-spark chamber apparatus capable to detect the Λ° produced in reactions of the kind

$$B^- + p \longrightarrow \Lambda^\circ + (\text{neutrals} \equiv X^\circ) \qquad (1)$$

and to measure its direction and momentum. According to the momentum of the incident particle B^- and to its nature (a beam of π^-, K^- or $\bar{p}$ can be alternatively used), the spectrometer will then be able to explore a definite region of the mass spectrum of the X° system (which will be one $S = +1$ meson, $S = 0$ meson, $S = +1$ antibaryon respectively).

This paper is mainly concerned with the study of the reaction

$$\pi^- + p \rightarrow \Lambda^\circ + (\text{neutrals} \equiv X^\circ) \qquad (1a)$$

but many general features we will discuss in the following sections, are common to all the reactions of type (1).

In its present version the experimental apparatus has been designed to detect and analyze the Λ°'s produced in the reaction (1a) in a momentum range from $\sim$ 250 to 1000 MeV/c and in an angular region between 0° and $\sim 55°$ around the beam direction. This means that for momenta of the incoming π^- in the range from 5 up to 10 GeV/c, the apparatus will allow the study of the invariant mass-spectrum of the X° system between ~ 1 GeV/c^2 and ~ 1.8 GeV/c^2 as a function of the p to Λ° four-momentum transfer Δ^2 (with good efficiency down to the minimum momentum transfer). The associate production

($X^o \neq K^o$, M^o = 498 MeV/c^2) will also be detected, but only in a limited range of Δ^2.

In the next section II we will briefly review the physical problems involved in the reaction (1a). Finally in section III the experimental apparatus will be described.

II. - Physics of the reaction $\pi^- + p \rightarrow \Lambda^o +$ (neutrals $\equiv X^o$) and problems in the mass spectrum of the X^o system

II. 1 - General features

The interest in studying the X^o mass system from the reaction

$$\pi^- + p \rightarrow \Lambda^o + (\text{neutrals} \equiv X^o) \qquad (1a)$$

rests mainly on the possibility of detecting quasi-two-body processes, like the ones sketched in fig. 1a.

The missing-mass technique allows for an accurate study of the production features of any given K^{*o} enhancement, by the measurement of its mass, width, possible structure, production cross section, Δ^2 dependence etc., as a function of the incoming π^- momentum. The decay features of the resonance under study will however remain mostly undetected: only an estimate of the associate number of the decay γ's (and therefore a separation between $K^o \pi^o$ and $K^o \pi^o \pi^o$ states) will be possible (see section III.2.2.).

The success of a missing-mass investigation clearly depends on the signal-to-noise ratio in the mass region of interest. The observed mass spectrum can in general be schematically apportioned between:

i) "phase-space" contributions (i.e. exhibiting no physical correlation among the outgoing particles).

ii) Quasi-two-body processes via "meson exchange" (as in fig. 1a, and in fig. 1b for the case $X^o \equiv K \pi \pi$ system). At sufficiently high energy, once the "peripheral" (or "Regge") production mechanism becomes dominant, the relative effect on the X^o mass spectrum of these quasi-two-body processes is in general strongly enhanced, as compared with (i), by a low- Δ^2 (from p to Λ^o) upper cut. This has been experimentally tested: e.g. at 6 GeV/c all the salient features of the X^o mass spectrum from reaction (1a) are practically untouched by a $\Delta^2 \lesssim 1 (GeV/c)^2$ cut which produces a strong "background" reduction.(1)

iii) "Baryon-exchange" contributions (corresponding to backward production of meson resonances), which are obviously ruled out by a low-momentum transfer cut.

iv) Quasi-two-body processes of the kind (see fig. 1c)

$$\pi^- + p \rightarrow Y^{*o} + K^{*o}(890)$$
$$\downarrow \qquad\qquad \downarrow$$
$$\Lambda^o + \pi^o \qquad K^o + \pi^o$$

These contributions are not strongly affected by a low- Δ^2 upper cut (low Δ^2 transferred from p to Λ^o means in practice low Δ^2 from p to Y^{*o}). However it is easy to show on kinematical grounds that, once the Δ^2 cut is applied and provided all the Y^{*o} decays are detected, the effective mass of the $(K^o \pi^o \pi^o)$ system (or similar ones) has a smooth ("phase-space"-like) structure, thus unable to simulate any peak effect in the X^o mass spectrum. This conclusion can be tested very well experimentally, for instance by looking at $\pi^+ p \rightarrow \Lambda^o K^+ \pi^+ \pi^o$. In this reaction in fact the diagram of fig. 2a is inhibited (as no $I = \frac{3}{2}$ resonace exists),

while a very strong and narrow $(\Lambda^o \pi^+)_{1385}$ signal is present (see fig. 2b). In this situation the total $(K^+ \pi^+ \pi^o)$ mass spectrum turns out experimentally[2] to be smooth and very similar to "phase-space".

v) A quite similar case is the one in which a Σ^o is produced at the bottom vertex (cfr. fig. 3), associated with a physical X^o state at the top vertex. In a region of low- Δ^2 from p to Λ^o (via Σ^o), the $(X^o + \gamma)$ spectrum, as it results from a Λ^o missing mass measurement, is then spread out over hundreds of MeV above the X^o mass, and it becomes lost in the general background (provided this process is not dominant, as compared with the process (1a); see below for the details).

vi) Finally, contributions from Deck-like processes (see fig. 1d) must be considered. This sort of diagrams have been first suggested[3] to account for the strong enhancements observed, since several years ago, in the $(K^*(890), \pi)$, (K, ϱ), (ϱ, π) mass distributions, immediately above the respective thresholds, whenever the production interaction is such that the target baryon (or nucleus) remains "untouched" by the interaction. For instance, in the case of "Q" production, this effect is observed in reactions like $K^- p \rightarrow p K^- \pi^+ \pi^-$ (or similar ones on unbroken nuclei), and not in processes like $K^- p \rightarrow n K^o \pi^+ \pi^-$ where a charge exchange process occurs at the baryon vertex. The situation is illustrated in fig. 4. An alternative and competitive mechanism to the standard production of resoances (cfr. fig.4a) can in fact be offered by a process like the one sketched in fig. 4b, where a diffraction scattering occurs at the bottom vertex. Diagram 4b experimentally shows up as an enhancement in the low region of the $K \pi \pi$ mass spectrum, due to purely

kinematical reasons. The presence of an elastic scattering process at the baryon vertex is then responsible for the dominance of Deck-like processes in the high energy region, where their cross section becomes roughly constant.

This model can be perfected (and more free parameters introduced)

- by considering other diagrams in which a K or a ϱ scatters off the proton, then adding coherently the corresponding amplitudes;
- by "reggeizing" the calculation, i.e. by involving in it the pion "trajectory" instead of the physical pion, etc. In this up to date version [4], the Deck-effect is in principle able to completely account for the observed phenomenology (i.e. regardless of contributions from diagrams like the 4a);
- finally by introducing, besides the purely kinematical contributions, real production mechanisms of reasonances according to the diagram of fig. 4c.

The basic philosophy of the present experiment, facing this very unclear and complex situation, is to look for a process like the reactions (1a) (cfr. also fig. 1) in which

i) the contributions from Deck-like diagrams (fig. 1d) are practically suppressed by the smallness and the energy dependence of the associated production bottom vertex;[5]

ii) it is experimentally ascertained[1],[2] that physical quasi-two-body processes (as in fig.s 1a, 1b) do take place (cfr. fig. 8c, from ref.1,2);

thus allowing for a more clear investigation on the K^{*o} mass spectrum.

II.2 - Problems in the mass spectrum of the X° system.

Almost all that is today experimentally known about the $I = \frac{1}{2}$ mass spectrum comes from bubble chamber experiments.

II.2.1 - At mass values above the well known K*(890) resonance, several experiments[6] on peripheral pion-production, allowing for a phase-shift analysis of the $K\pi$ system, give indications of a possible S-wave $K\pi$ resonant state around $M° \sim 1.0-1.1$ GeV/c^2. Also the $K\pi$ mass spectra obtained in some other experiments[7] seem to give further, but rather contradictory, marginal evidence for the existence of such a resonant state, together with another one around ~ 1160 MeV/c^2. However the situation in this region of mass is still not clear at all.

The present missing mass experiment, which allows one (see sect. III.2.2) to count the photons associated with the $\Lambda°$, should be able to separate the contribution of possible $K° \pi°$ states from the $K° \pi° \pi°$ ones.

II.2.2 - The "Q" region ($1.0 \leq M° \leq 1.4$ GeV/c^2)

In any experiment concerning reactions of the type:

$$K^{\pm} + p \rightarrow p + (K \pi \pi) \qquad (2)$$

for momenta of the incident kaons greater than 4 GeV/c a broad prominent peak (called the "Q" effect) has been observed in the region between ~ 1.0 and 1.4 GeV/c^2 of the $(K \pi \pi)$ system mass spectrum[8],[9] (see e.g. fig. 5). The main features of this big "bump", which are confirmed by all the experiments, can be summarized as follows:

i) it includes (and obscures) a contribution, rapidly

decreasing with increasing energy, of the well known K*(1420) resonance.

ii) As is true for the K*(1420), the overall "Q" effect has isospin I = $\frac{1}{2}$ and appears in a decreasing order of importance in the three (K*(890),π), (ϱ, K) and (K π π) channels. It is however impossible from the available experimental data to make a consistent evaluation of the relative decay branching ratios of the "Q" interpreted as a definite state.

iii) Changes in the incident $K^{\pm}$ momentum, as well as selection of different regions of the four-momentum transfer Δ^2 or of particular decay configurations, seem to produce mass splitting of the "Q" bump. However there is on this point a large degree of inconsistency between different experiments, while the significance of the various observed effects remains questionable, due to the statistical errors.

iv) A recent analysis[9] of all the available experimental data shows that they are incompatible with a single Breit-Wigner shape; on the other hand if they are fitted to an incoherent sum of two (not resolved) Breit-Wigner's, then the resulting masses and widths tend to agree among several experiments, and to become quite constant, above $\sim$ 6 GeV/c incident K^+ momentum (see fig. 6).

v) Finally all the attempts to spin analyze the (K*(890),π) channel indicate, or are consistent with, a dominant $J^P = 1^+$ assignment.

All this phenomenology is not inconsistent with what we expect on the basis of our present understanding of strong interactions. In fact any quark model for the hadron spectrum predicts the existence of at least two $J^P = 1^+$ meson nonets of opposite C. The presence of the I = $\frac{1}{2}$ members of the two

nonets, say K^A and K^B, is expected to give rise to the following effects:

i) an SU(3) mixing leading to new physical masses K' and K" and new widths for the allowed channels;

ii) a physical interference between K' and K" according to their production and decay properties. As an example of such an effect, fig. 7 shows some possible interference patterns calculated by Goldhaber.(10)

On the other hand "diffraction dissociation" processes like the generalized Deck-effect (see sect. II.1) are known to take place, and they are themselves able to result into mass enhancements like the observed "Q" structure. This kind of "background", characterized by $J^P = 1^+$ final states, will contribute to the process (2) with a set of amplitudes possibly comparable and coherent with the K' and K" ones. Therefore it may give rise to an unpredictable interference behaviour as a function of the incident kaon energy and the four-momentum transfer to the baryon. Such a complicate interference could be responsible for the present difficulties in extracting simple and consistent conclusions from the existing experimental data.

A different approach to the same problem has been used in a large (20 events/μbarn) bubble-chamber experiment(1),(2) studying the π^- p interactions at 6 GeV/c incident π^- momentum. Fig. 8a shows the invariant mass spectrum of the $(K\pi\pi)^\circ$ system from the reaction

$$\pi^- + p \rightarrow \Lambda^\circ + (K\pi\pi)^\circ \qquad (3)$$

for the two channels $\Lambda^\circ K^+\pi^-\pi^\circ$ and $\Lambda^\circ K^\circ\pi^+\pi^-$. Around 1300 and 1440 MeV/c^2, two prominent peaks are observed above a

"honestly" smooth background. It is interesting to note the total absence of any enhancement below the $K\pi\pi$ mass value 1.2 GeV/c^2, where the ordinary Deck-like processes still contribute a very large cross section. A second interesting feature of the data is shown in figs. 8a and 8b comparing the $K\pi\pi$ mass spectra with and without the cut on the momentum transfer from p to Λ°, respectively. It is immediately seen that the contribution to the two peaks due to events with momentum transfer $\Delta^2 > 1$ (GeV/c)^2 is practically negligible, thus confirming (cfr. sect. II.1) the quasi-two-body nature of the process responsible of their production. The missing mass spectrum from reaction (1a) as observed in the same experiment[1] is also given in fig. 8c, where a Δ^2 cut at 1 (GeV/c)^2 has been applied. The lack of statistics clearly prevents any significant conclusion to be drawn.

II.2.3 - The K*(1420) resonance

The next good reason to investigate the $K^{*\circ}$ mass spectrum with good statistics and resolution is to search for a possible mass splitting of the K*(1420).

This meson belongs to the same well known 2^+ multiplet as the A_2 meson does: all the relations between masses, widths and branching ratios of its components being in good agreement with the SU(3) scheme. On the other hand, the rather well established[11] mass splitting of A_2 opens now the question of whether other particles of the nonet might also exhibit a similar behaviour.

II.2.4 - The "L" region ($1.6 \leqslant M^\circ \leqslant 1.8$ GeV/c^2)

In the mass region between ~ 1.6 and 1.8 GeV/c^2 several experiments[8],[12] have observed definite structures in the $K\pi\pi$ mass spectrum (the "L" meson). The effect is

somehow similar(*) to the "Q", although it is much less pronounced and poorly studied as yet.

Different experiments seem to indicate possible splittings in "subresonances". Attempts have also been made to account for all or part of the effect through a Deck-like mechanism and related diagrams involving this time a K*(1420), instead of the K*(890) as in the "Q" case. Also the existing preliminary evidence for a $J^P = 2^-$ assignment would be in agreement with such hypothesis. On the other hand there are experimental data claiming for "L" contributions to decay modes different from (K*(1420),π), thus inferring the presence of at least some "resonance production" content in the "L" region. It appears that the phenomenological situation is, as yet, even less clear than for the "Q" effect.

III. - The Λ° Missing Mass Spectrometer.

III. 1 - General features

In its present version the experimental apparatus is designed to detect and analyze the Λ°'s (of momentum between $\sim$ 250 and 1000 MeV/c) produced in the reaction

$$\pi^- + p \rightarrow \Lambda^\circ + (\text{neutrals} \equiv X^\circ) \qquad (1a)$$

the incident pion momenta ranging from $\sim$ 5 up to $\sim$10 GeV/c. This means that low momentum transfer (i.e. meson exchange) processes will be automatically enhanced by the trigger, over

(*) A proof of this similarity could lie in the fact that both the "bumps" appears to be produced coherently on deuterium (Cfr. ref. 13).

the contributions from phase-space and different physical processes discussed in sect. II.1.

Due to the upper cut in the momentum of the Λ° detected, the corresponding observed X° mass spectra will be cut on the high mass side. For instance at 10 GeV/c incident beam momentum the X° mass spectrum for the reaction (1a) will be cut starting at $M^\circ \sim 1.8$ GeV/c^2 (M° = invariant mass of the X° system). On the other hand Λ° momenta below $\sim$ 250 MeV/c will not be accepted by the apparatus. Nevertheless this still allows M° masses larger than about $\sim$ 1.0 GeV/c^2 to be detected with good efficiency down to their minimum momentum transfer. Thus it will be possible to make a careful dynamical study of the X°'s production processes(*) in the 1.0–1.8 GeV/c^2 mass region.

An important feature of the experiment is that in the production of physically defined states X° (via the reaction (1a)) the p to Λ° momentum transfer distribution is expected to be at high energy practically independent of the incident beam momentum. This means that the efficiency of the apparatus for detecting a given X° state will be nearly constant as the incident π^- beam momentum is varied. This is foreseen to be very important in disentangling contributions due to possibly contiguous resonances by the study of their different production behaviour as a function of the incident beam momentum and of the momentum transfer in the production reaction.

Finally the apparatus (as we will see in sect. III.2.2) is such that it will have also a good efficiency for detecting the γ's associated with each event from reaction (1a), thus allowing further information of the different X° states.

(*) Moreover if for a given quasi-two-body process the production cross section is large enough, the corresponding polarization will also be measurable.

III.2 - The Spectrometer

Since one must detect low momentum Λ°'s produced in the reaction (1a) and measure their direction and energy, one first has to use a "neutral trigger" having its anticoincidence counter surrounding the H_2 target at the closest distance possible. Then the direction of both of the charged decay products of the Λ° (i.e. π^- and p), and the momentum of at least one of these, have to be measured in order to reconstruct the production angle and momentum of the Λ° .

III.2.1 - Kinematics

For a better understanding of the problems of the experimental apparatus we will first briefly discuss the kinematics of the reaction (1a).

For each K*° mass produced in reaction (1a) a minimum value of the proton to Λ° momentum transfer, Δ^2_{min}, (i.e. of the Λ° momentum in the laboratory, $p_{\Lambda min}$) is allowed. Fig. 9 shows the behaviour of $p_{\Lambda min}$ and $\theta_{\Lambda max}$ (maximum angle between the Λ° and the π^- beam direction in the laboratory system) for several K*° mass value as a function of the incident beam momentum, $p_{\pi in}$.

The Λ° decay protons have momenta and angles, in the laboratory system, not very far from the ones of their parent Λ°'s. Therefore the apparatus must detect protons down to $\sim$ 300 MeV/c momentum in order to explore the minimum momentum transfer region for low M° masses, while the angle at which protons are detected also define the angular Λ° acceptance (the maximum possible p-Λ° angle is $\sim 20°$).

As a result of the previous considerations one has to detect and momentum analyze protons of momenta between 300 and 1000 GeV/c emitted inside a cone of $\sim$ 55°-60° aperture around the beam direction.

III.2.2 - The experimental apparatus

A schematic view of the apparatus is given in fig.10. A counter hodoscope placed in the focal plane of the beam-momentum-analysing magnet allows one to achieve a better than $\sim \pm .5\%$ definition of the π^- incident beam momentum. A coincidence between counters $B_1 \cdot B_2 \cdot \bar{B}_3 \cdot \bar{B}_T \equiv B$ monitors the incoming and interacting particle. T is a thin, mylar-walled H_2 target, $\sim$ 20 cm long, completely surrounded by a system of anticoincidence counters C_1 which are placed very close ($\lesssim 1$ cm) to it. $C_2^i (i = 1 \ldots 9)$ are nine triangular counters arranged as sectors of a circle normal to the beam direction.

The C_2^i's counters are put in coincidence with the beam, B, and therefore they define the maximum decay path for the Λ° and the maximum accepted angle of its decay proton ($\sim 55^\circ$). Furthermore the main trigger, "T_A", requires that two (and no more than two) different sectors C_2^i give a pulse. This condition selects "good" Λ°'s by rejecting, at the trigger level, a large fraction of Λ°'s with small decay opening angle or decay plane containing the beam direction, which give poor resolution in the reconstruction of the events as we will see later on. An alternative trigger, "T_B", requires only one sector C_2^i to give a pulse corresponding to the decay proton, while the associated decay pion is detected by one of the two C_π telescopes.

After the C_2^i counters a 3 cm thick water Čerenkov counter, Č, is put in anticoincidence in the trigger (*). This counter rejects any pion and proton faster than $\sim$160 and $\sim$1000

(*) In order to avoid stopping 300 MeV/c momentum proton, the thickness of the Čerenkov counter is limited to 3 cm. Nevertheless if the Čerenkov light is seen by eighteen 150AVP phototubes, the efficiency, as measured with π^- of 900 MeV/c momentum, turns out to be larger than $\sim$ 98% (cfr. ref.14).

MeV/c respectively.(*)

The master trigger of the experiment is therefore given by:

$$T \rightarrow \begin{cases} T_A \equiv B_1 B_2 \bar{B}_3 \bar{B}_T \bar{C}_1 (C_2^i C_2^j) \bar{\bar{C}} \\ T_B \equiv B_1 B_2 \bar{B}_3 \bar{B}_T \bar{C}_1 C_2^i C_\pi \bar{\bar{C}} \end{cases} \qquad (4)$$

The Aluminum plate spark chambers BCH_1 and BCH_2 will measure the direction of the incident beam. WG is an optical 10 cm wide gap wire chamber used to reconstruct the direction of both the decay products of the Λ°. As we will see, a high spatial resolution and a good detection efficiency for two simultaneous tracks with a large angular difference are fundamental requirements to obtain the desired resolution in M° mass. For this reason we make use of a wide gap chamber working in such a way (i.e. near the "streamer" condition) as to allow the detection of both particles with good efficiency and good spark quality (thin and uniformly visible tracks). The WG chamber is seen in four stereo views, in order to avoid ambiguities and optimize precision during the reconstruction process.

RCH_i's are a set of range chambers in which the protons come to rest. They consist of 48 (Al and Fe) plates whose thickness was planned to give constant momentum resolution $\Delta p/p \lesssim 2\%$. Because of the large amount of Fe ($\sim$ 7 radiation lengths), the range chambers have also a good efficiency in con

(*) The upper limit on the proton momentum closely corresponds to a similar cut in the Λ° momentum, and then in the $\Delta^2(p \rightarrow \Lambda^\circ)$. Fast decay pions correspond to small-aperture Λ° decays, already antiselected by the trigger, leading to poor resolution.

verting γ's within a $\sim 55°$ cone around the beam direction. This provides an efficient count of the γ rays associated with each detected event, thus allowing discrimination of different X^o states.

The requirement that the decay protons have to stop in the range chamber defines the accepted proton momentum interval. The lower momentum limit corresponds to a range equal to the amount of material (mainly the $\check{C}$ counter) in front of the range chambers. It turns out to be ~ 300 MeV/c. The upper momentum limit, corresponding to the total amount of material of the range chambers, is ~ 1000 MeV/c.

III.2.3 - Reconstruction of the events and mass resolution

The reconstruction of the M^o mass value for any given event will proceed in the following manner. The two trajectories of the decay products of the Λ^o (reconstructed from their tracks in the wide gap spark-chamber) are fitted to a common decay plane. Extrapolation of the two trajectories on this plane determines the Λ^o decay vertex. The intersection of the decay plane with the beam direction (as measured by the BCH_i's spark chambers) gives the production vertex. Because the proton momentum is directly measured in the experiment, at this point only p_Λ and $p_{\pi^-,dec}$ remain unknown. Energy and momentum conservations allow then a 2-constraints fit to the Λ^o momentum and production angle.

The M^o missing mass is then give by

$$M^{o2} = (E_{TOT} - E_\Lambda)^2 - p_\Lambda^2 - p_{\pi in} + 2 p_{\pi in} p_\Lambda \cos\theta_\Lambda \qquad (5)$$

where $E_{TOT} = \sqrt{p_{\pi in}^2 + m_\pi^2} + M_p$ is the total energy in the

laboratory system and E_Λ is the total Λ° energy.

The mass resolution ΔM° depends on the beam momentum definition, $\Delta p_{\pi in}$, and on Δp_Λ and $\Delta\theta_\Lambda$, which are the errors associated with the Λ° momentum and angle as obtained by the 2-constraints fit from the quantities we experimentally measure (i.e. the direction of both the Λ° decay products and the proton momentum p_p). Δp_Λ and $\Delta\theta_\Lambda$ in turn vary with the specific Λ° decay configuration of each event (i.e. with the distance between the production and the decay vertices, with the angles of the decay products, and with the proton momentum). However we can evaluate the order of magnitude of the average indetermination in measuring $p_{\pi in}$, θ_π, θ_p and p_p.

Assuming

$$\Delta p_{\pi in} / p_{\pi in} \sim 0.5\ \%$$

$$\Delta\theta_{\pi^-,dec} = \Delta\theta_p \sim 3\ \text{mrad}\ (*) \qquad (6)$$

$$\Delta p_p / p_p \sim 2\ \%$$

we obtain the average ΔM° distributions shown in fig. 11: the resulting half-widths-half-maximum are of the order of $\sim \pm 6\ \text{MeV/c}^2$. Besides the trigger requirements, no further restrictions on the decay configuration were set in the Montecarlo calculation. By appropriately selecting the type of Λ° decay configuration one can further improve the M° mass

(*) In a preliminary "test run" performed on a low energy beam at CERN, we have checked that the wide-gap chamber allows the detection of the Λ° decay products with the quoted angular resolution (cfr. ref. 14).

resolution. The effect of such a selection can be then easily and exactly evaluated in terms of the well known Λ° decay parameters.

Another problem of the analysis concernes the protons that undergo nuclear interactions in the range chamber. In this case the fitting procedure uses an incoherent experimental value of the proton momentum. Two cases are then possible:

a) the reconstruction fails and the event is rejected by the fit;

b) the event is not rejected and a wrong M° value is obtained.

These two effects have been estimated by a Montecarlo simulation of the experimental situation. In the case a) the inefficiency turns out to be small ($\sim$ 10% of the events are rejected in the analysis). Class b) amounts to about 15% of the events which have given a "good" fit. As it can be seen in fig. 12, these events result in a smooth "background" which is spread over a ~ 300 MeV/c^2 mass interval, while the h.w.h.m. of the average ΔM° distribution is about ± 6 MeV/c^2 (cfr. fig. 11).

III.2.4 - Detection efficiency

The detection efficiency of the apparatus at 6 and 10 GeV/c incident pion momenta is shown in figs. 13, for both "T_A" and "T_B" triggers (cfr. sect. III.2.2, eq. (4)), as a function of the M° mass (fig.13a) and of the momentum transfer Δ^2 (fig.13b). The efficiency has been computed by a Montecarlo, using the Čerenkov counter efficiency (as a function of the momentum) and the appropriate cuts in angles and momenta of the detected particles. At 6 GeV the events have been generated according to the results of a bubble chamber experiment[1),(2)]; at 10 GeV/c we have made the assumption that the p to Λ°

momentum transfer distribution has the same shape as at 6 GeV/c.

From fig. 13a it can be seen that the efficiency corresponding to the "T_A" trigger mode is reasonably smooth over the 1.0–1.8 GeV/c^2 interval of M° mass. When M° is lower than $\sim$ 1 GeV/c^2 the efficiency falls down; but, besides the existence of a "T_B" trigger mode, the relatively large value of the associate K° and K*(890) resonance production cross section will allow us to collect a sizeable number of Λ° corresponding to these processes. Such events will provide a very useful calibration of the whole experimental set up for both the absolute mass scale calibration and the mass resolution. Finally, it is to be noticed that the M° dependence of the detection efficiency basically rests on the geometrical acceptance of the apparatus and on the well known decay properties of a Λ° of a given momentum; the corresponding weight to be attributed to each event will therefore be exactly evaluable across all the M° mass spectrum.

We have also studied the detection efficiency of the apparatus if the decay proton momentum analysis were performed with a magnet instead of using a range spark-chamber system. Fig. 14 shows the result of such a calculation assuming the characteristics of a magnet available at CERN (gap dimensions: 50x50x50 cm^3). By comparing figs. 13 and 14 we can conclude that in the M° mass region we are interested in ($\sim 1.0 \leqslant M^\circ \lesssim 1.8$ GeV/c^2), the use of a proton momentum analyzing magnet is not recommended, due to the strong dependence of the efficiency on M° and Δ^2 introduced by the limitations in the accepted solid angle. On the other hand magnetic analysis appears to be the best method for investigating the large K*° mass region ($\gtrsim 1.7$ GeV/c^2).

III.2.5. Counting rates

The counting rate of the apparatus is given by

$$n = I N \ell \varrho \sigma_{eff} \tag{7}$$

where

n = number of trigger per machine burst,

I = incident flux (number of incident particles per burst),

N = Avogadro's number,

ℓ = target length,

ϱ = liquid hydrogen density,

σ_{eff} = effective cross section = $\int \frac{d\sigma}{dM^\circ d\Delta^2} \varepsilon(M^\circ, \Delta^2) dM^\circ d\Delta^2$.

$\varepsilon(M^\circ, \Delta^2)$ is the detection efficiency of the apparatus parametrized in terms of M° (i.e. the X° system effective mass) and Δ^2 (i.e. the $p \rightarrow \Lambda^\circ$ four-momentum transfer squared).

At 6 GeV/c incident π^- momentum, and in the interval of X° mass between 1.0 and 1.8 GeV/c^2, the expected number of events from reaction

$$\pi^- + p \rightarrow \Lambda^\circ + (\text{neutrals} \equiv X^\circ) \tag{1a}$$

detected by the Λ° missing mass spectrometer turns out to be

$$n = 0.4 \text{ triggers/burst} \quad (1.0 \leqslant M^\circ \leqslant 1.8 \text{ GeV}/c^2)$$

with a beam intensity $I = 1.5 \cdot 10^5$ π's/burst and a 20 cm long H_2 target. This number has been calculated on the basis of the available bubble chamber data (cfr. refs. 1, 2 and fig. 8c).

At higher π^- momenta (up to 10 GeV/c) the detection efficiency of the apparatus, as determined under the assumption of a $\Delta^2(p \rightarrow \Lambda^\circ)$ distribution similar to the one at 6 GeV/c

incident pion momentum, remains practically the same (cfr. sect. III.2.4). But up to now we don't have any experimental indication on the value of the cross section for reaction (1a).

III.2.6 - Background

The background of the experiment can be divided into two classes:

i) "trigger background", that is events which give a trigger but are eliminated by the data analysis;

ii) " Σ° background", that is events due to the reaction

$$\pi^- + p \longrightarrow \Sigma^\circ + X^\circ \longrightarrow \Lambda^\circ + X^{\circ\prime} \quad (\equiv X^\circ + \gamma) \qquad (8)$$

Trigger background

The most important processes that can trigger the experimental apparatus are the following:

i) π^-_{in} interactions in the target that give rise to charged particles. If no vetoed by both C_1 and $\check{C}$, they can trigger two of the C_2^i counters, thus resulting in a master trigger.

ii) $\pi^- + p \longrightarrow n + \pi^\circ$'s interactions. One or more of the π° decay γ's can convert in the material in front of C_2^i and, if the resulting electrons are not vetoed by $\check{C}$, they can give a pulse in two different C_2^i sectors.

iii) π^- interactions producing $K^\circ + \bar{K}^\circ + \pi^\circ$'s. If the K° decays after the C_1 counter and the decay charged pions fail to be vetoed by the $\check{C}$, they can give rise to a master trigger.

Assuming:

- inefficiency of the anticoincidence $\bar{C}_1 \leq 10^{-3}$,
- inefficiency of the $\check{C} \leq 2\%$, (14)
- total amount of material in which γ's can convert $\leq 2 \cdot 10^{-2}$ R.L.

(mainly the WG spark chamber and the target wall) (*), it can be shown that, even under further pessimistic assumptions, the number of triggers due to these processes is less than $\sim$ 30% of the "good" events (from reaction (1a)). Of course all this 30% background can be easily eliminated during the analysis.

Σ° background

As far as the Σ° background is concerned, the present apparatus is unable to distinguish these processes from the ones we want to study (reaction (1a)). However:

i) the cross sections for quasi-two-body processes in channels $\pi^- + p \rightarrow \Sigma^\circ + K^*$ are lower than the corresponding ones in which a Λ° is directly produced, and the same is generally true also for K^- induced reactions;

ii) a narrow peak in the X° mass produced via reaction (8) will be spread over several hundred MeV of the mass spectrum, once the events are analyzed as if a $M^{\circ\prime}$ system were produced associated to a Λ° in a reaction of type (1a). This means that events from channels (8) will results only in a smooth "background" when one looks for reasonably narrow $K^{*\circ}$ resonances produced via reaction (1a).

In the first half of 1970, we have experimentally tested the Λ° missing mass spectrometer apparatus (only the range chambers were not in place) by studying the associate K° production in a low energy π^- beam at CERN. The results of such a test run[14] assure we are able to achieve the required spacial resolution and a very good rejection of the background.

The Λ° missing mass spectrometer will start to run in a high energy π^- beam at CERN, near the end of 1971.

---

*) This can be practically achieved by using planes of thin wires as WG chamber plates.

REFERENCES

1) - Q.W.Lai, private communication of unpublished results from the experiment quoted in ref. 2.

2)-D.J.Crennel et al., Phys.Rev.Letters 19, 44 (1967).

3) - R.T.Deck, Phys.Rev.Letters 13, 169 (1964).

4) - E.L.Berger, Phys.Review 166, 1525 (1968).

5) - K.W.Lai and J.M.Shpiz, Phys.Review 182, 1536 (1969).

6) - Proceedings of the 1969 Argonne Conference on $\pi\pi$ and $K\pi$ interactions, Argonne National Laboratory May 1969: several papers.

7)-Review of Particles Properties in Phys.Letters 33B, 1, (1970); and
- Firestone et al., UCRL-20091, 25 August 1970.

8) - Proceedings of the Heidelberg Conference on Elementary Particles, Heidelberg September 1967, pag.11;
- Proceedings of the 14th International Conference on High-Energy Physics, Vienna September 1968, pag. 91;
- Proceedings of the Lund International Conference on Elementary Particles, Lund June-July 1969, pag. 313.

9) - A.Firestone, UCRL-19846, June 1970.

10) - G.Goldhaber, Phys.Rev.Letters 19, 976 (1967).

11) - R.Band et al., Phys.Letters 31B, 397 (1970).
- M.Basile et al., Lettere al Nuovo Cimento IV, 838 (1970).
- Barbaro-Galtieri, UCRL-19865, July 1970.

12) - A.Barbaro-Galtieri et al., Phys.Rev.Letters 22, 1207 (1969);
- J.Bartsch et al., Phys.Letters 33B, 186 (1970).

13) - D.Denegri et al., Phys.Rev.Letters 20, 1194 (1968).

14)-I.Bruner, U.Dore, P.Guidoni, I.Laakso, G.Martellotti, G.Marini, F.Massa, G.Piredda, P.Pistilli, M.Severi: "Results of a test run of a Λ^o missing mass spectrometer, near single K^o production threshold" - IFU Internal Report, to be published.

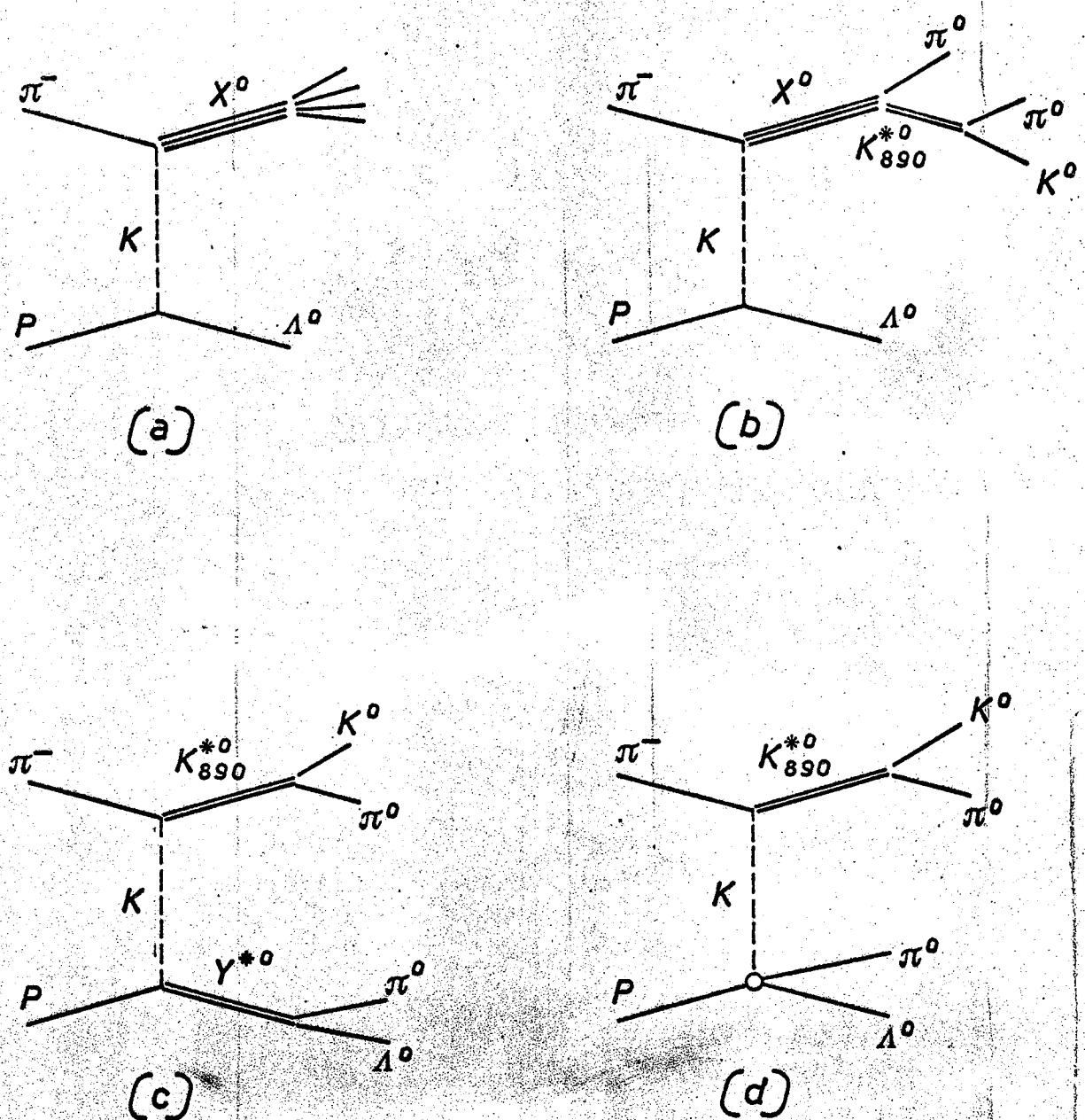
π⁻
X⁰
K
P
Λ⁰
(a)
π⁻
X⁰
π⁰
K*⁰₈₉₀
π⁰
K⁰
K
P
Λ⁰
(b)
π⁻
K*⁰₈₉₀
K⁰
π⁰
K
P
Y*⁰
π⁰
Λ⁰
(c)
π⁻
K*⁰₈₉₀
K⁰
π⁰
K
P
π⁰
Λ⁰
(d)

FIG. 1

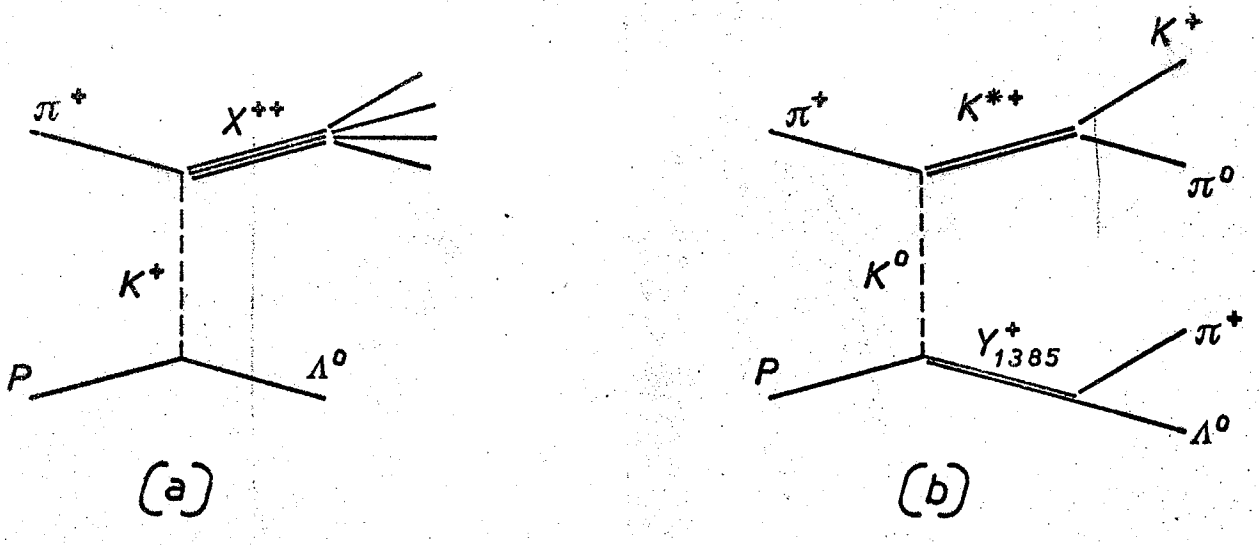

FIG. 2

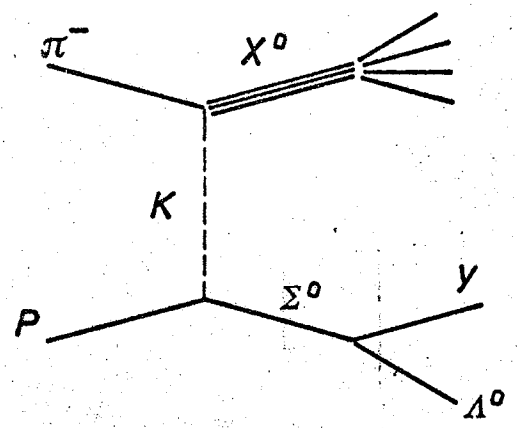

FIG. 3

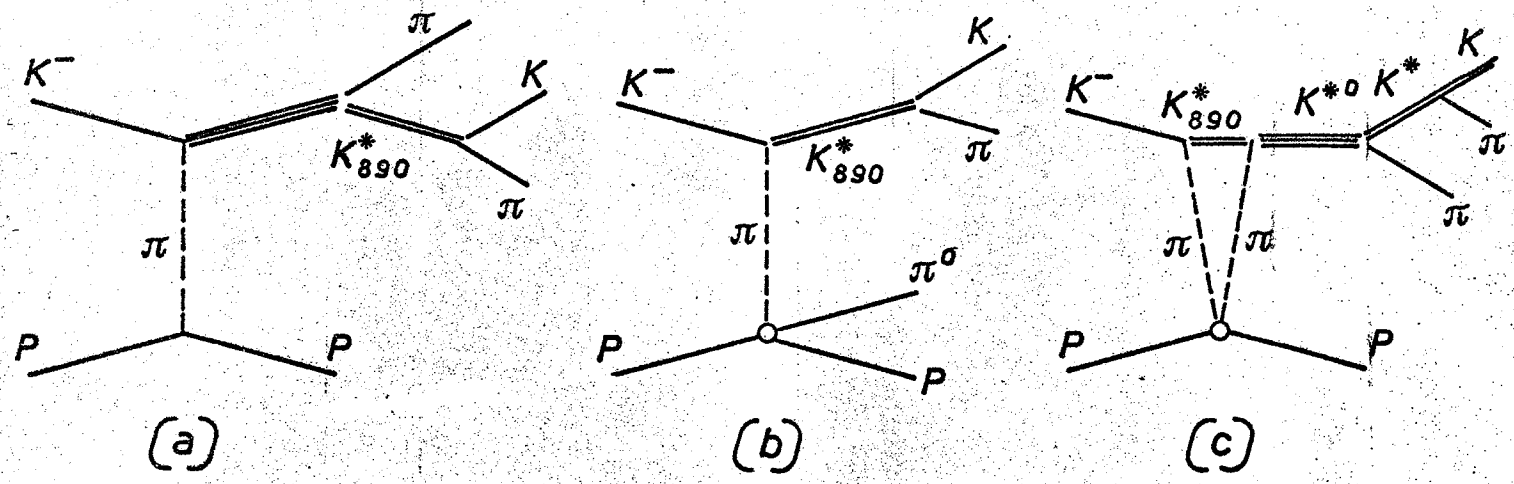

FIG. 4

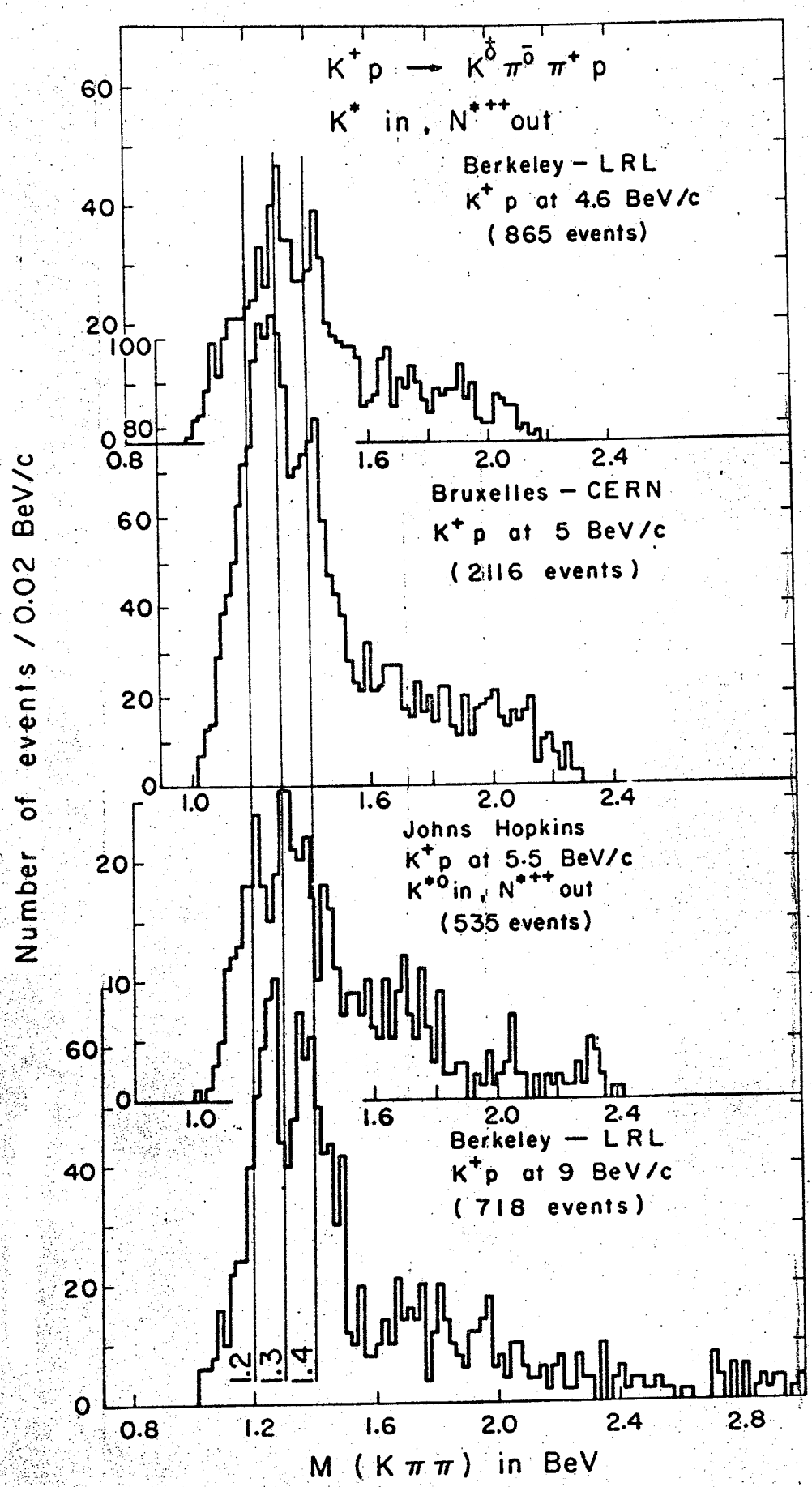

Fig. 5. Comparison of Kππ effective mass distribution found in four Kp experiments.

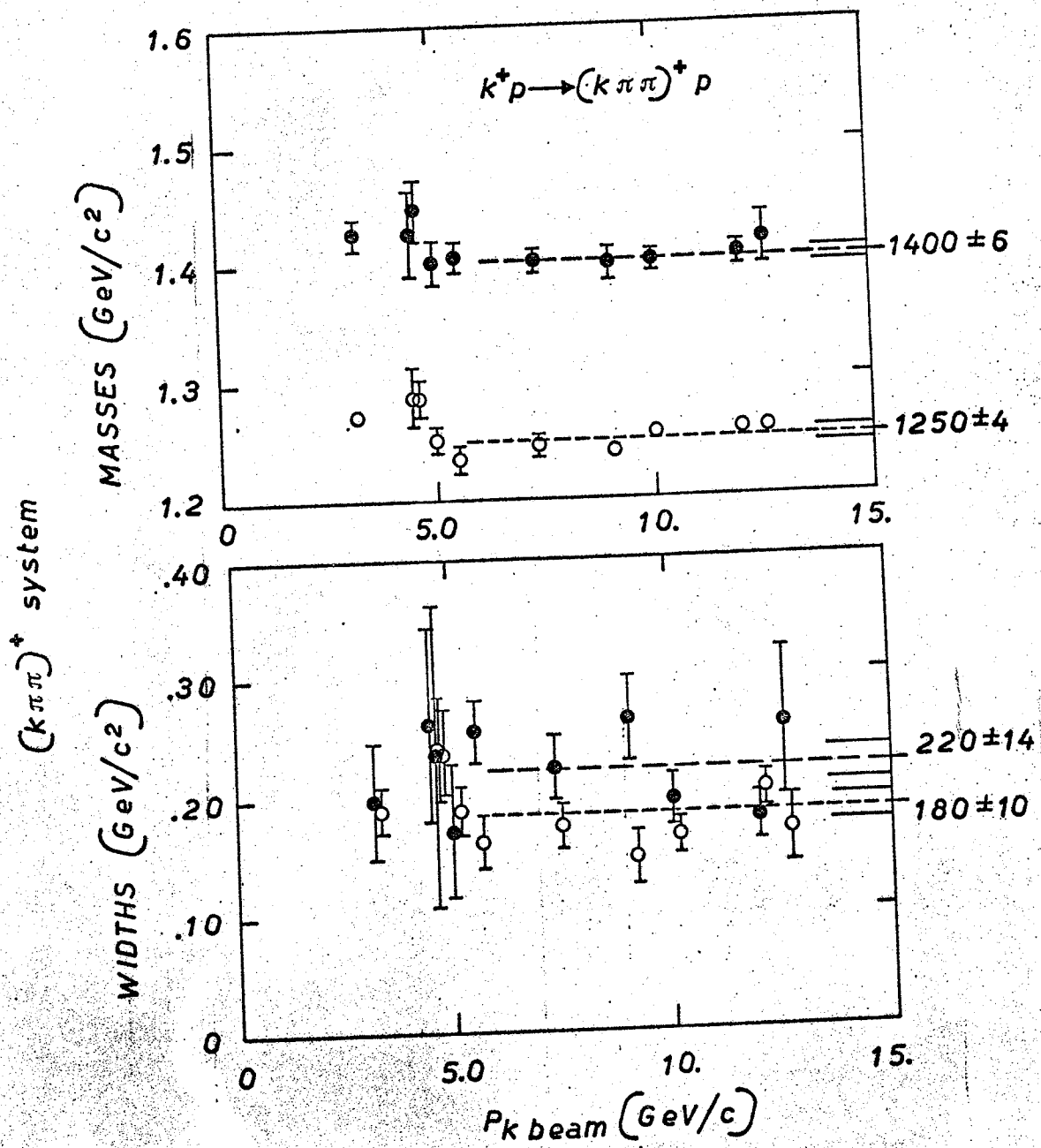
$k^+p \rightarrow (k\pi\pi)^+ p$
MASSES (GeV/c²)
1.6
1.5
1.4
1.3
1.2
1400 ± 6
1250 ± 4
0
5.0
10.
15.
WIDTHS (GeV/c²)
.40
.30
.20
.10
0
220 ± 14
180 ± 10
$(k\pi\pi)^+$ system
P_k beam (GeV/c)

FIG. 6

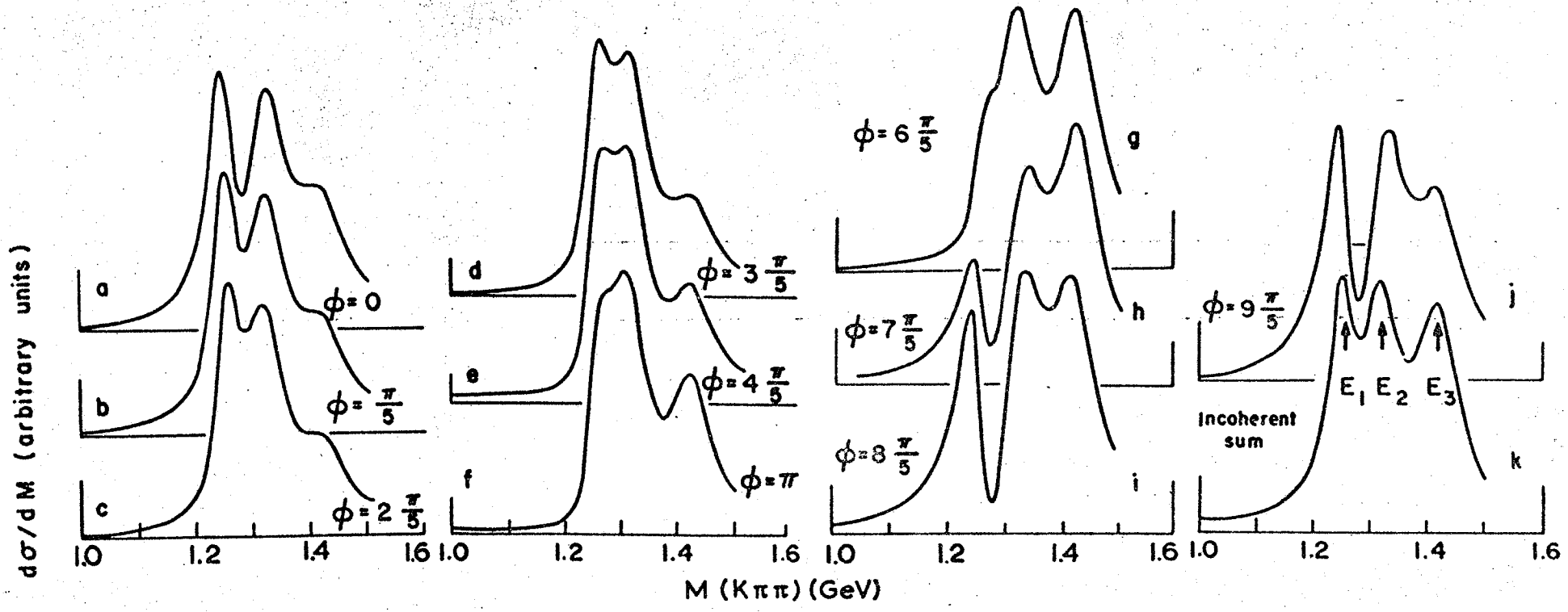

Fig. 7. Calculations by Goldhaber of $K\pi\pi$ mass distributions for two coherent 1^+ states at 1250 and 1320 plus an incoherent 2^+ state at 1420, as the relative phase of the two equal amplitude 1^+ states varies.

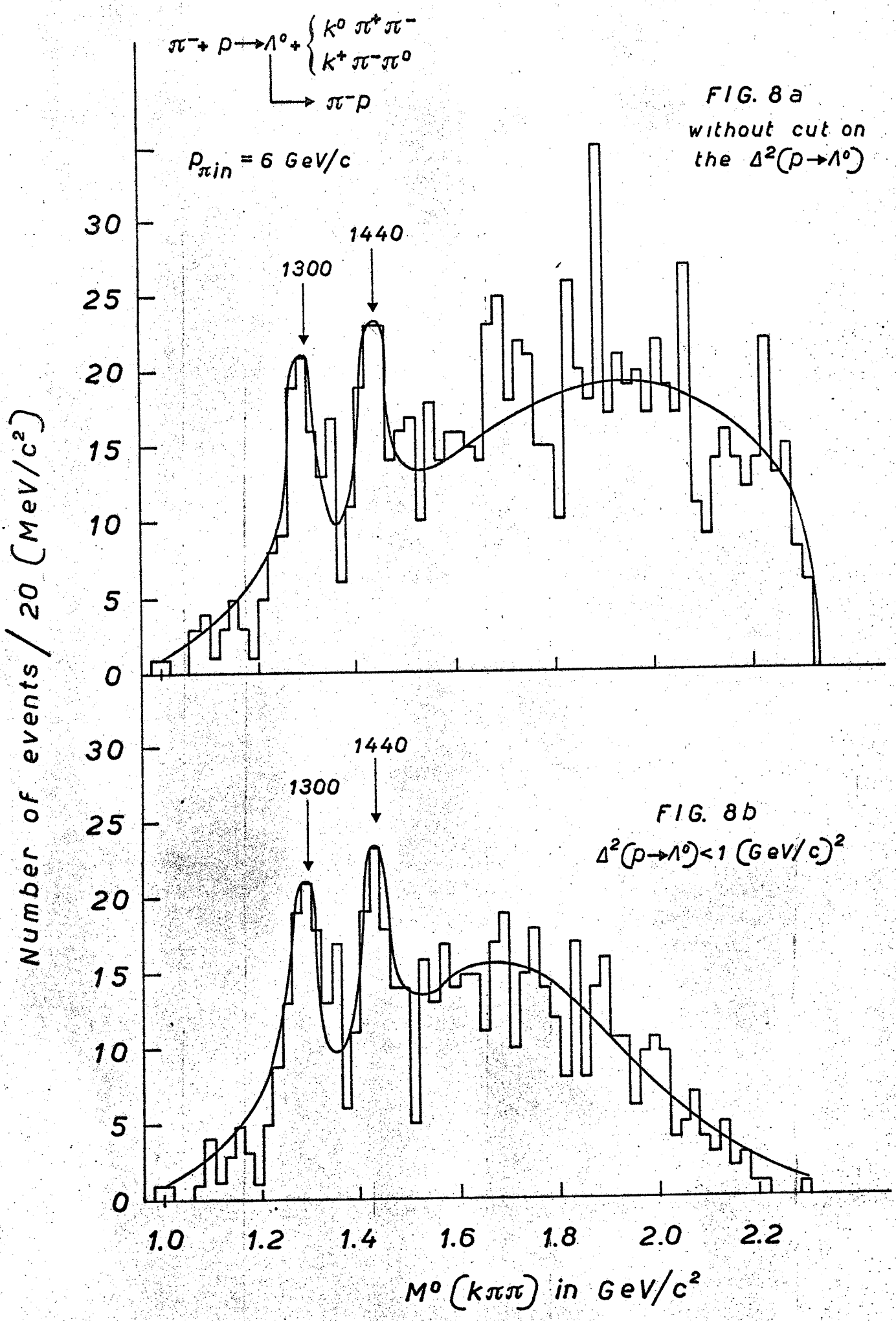

FIG. 8a
without cut on
the $\Delta^2(p \rightarrow \Lambda^0)$

FIG. 8b
$\Delta^2(p \rightarrow \Lambda^0) < 1$ (GeV/c)²

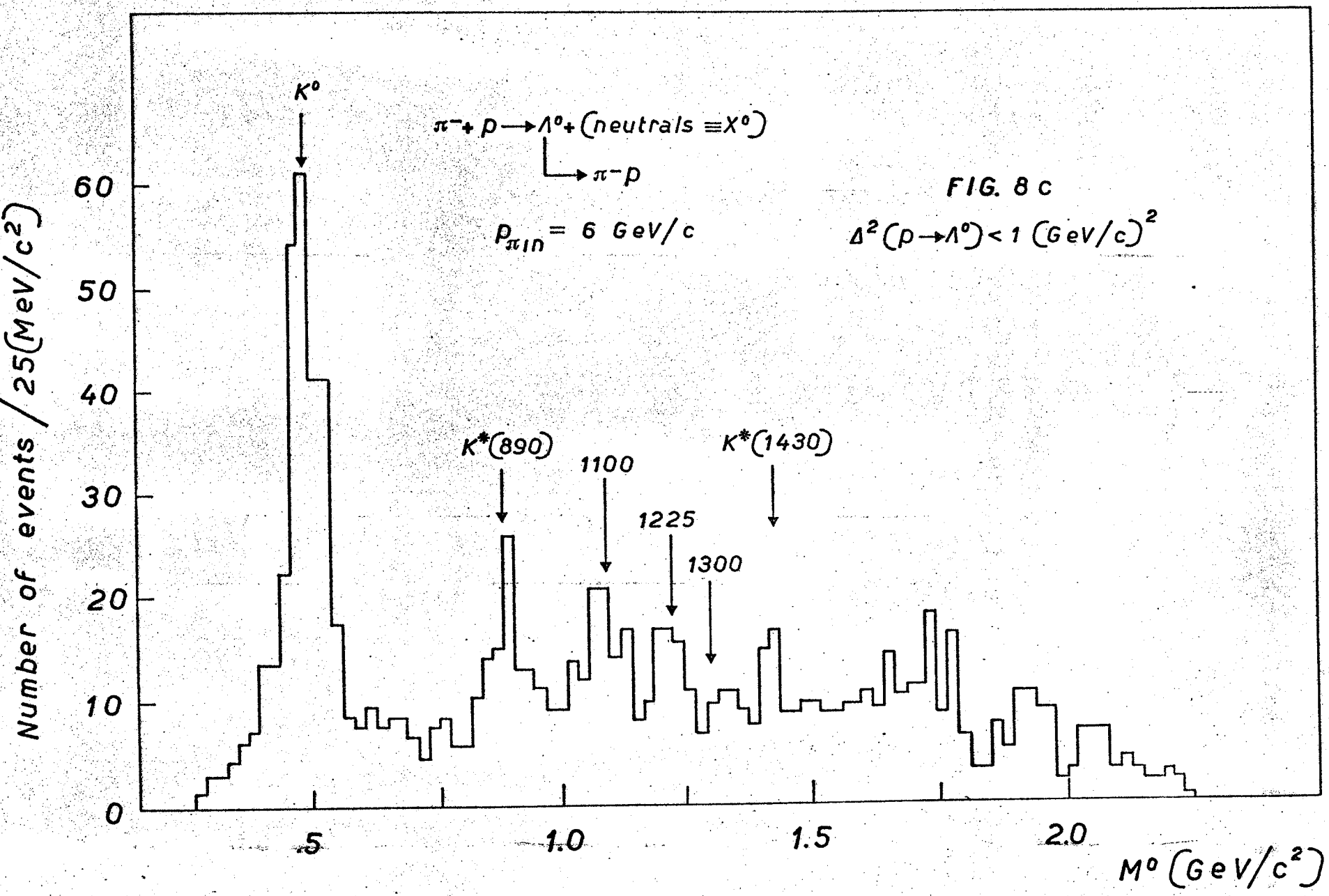
K°
π⁻ + p → Λ° + (neutrals ≡ X°)
→ π⁻ p
P_πin = 6 GeV/c
Δ²(p → Λ°) < 1 (GeV/c)²
K*(890)
1100
1225
1300
K*(1430)
Number of events / 25(MeV/c²)
60
50
40
30
20
10
0
.5
1.0
1.5
2.0
M° (GeV/c²)

FIG. 8 c

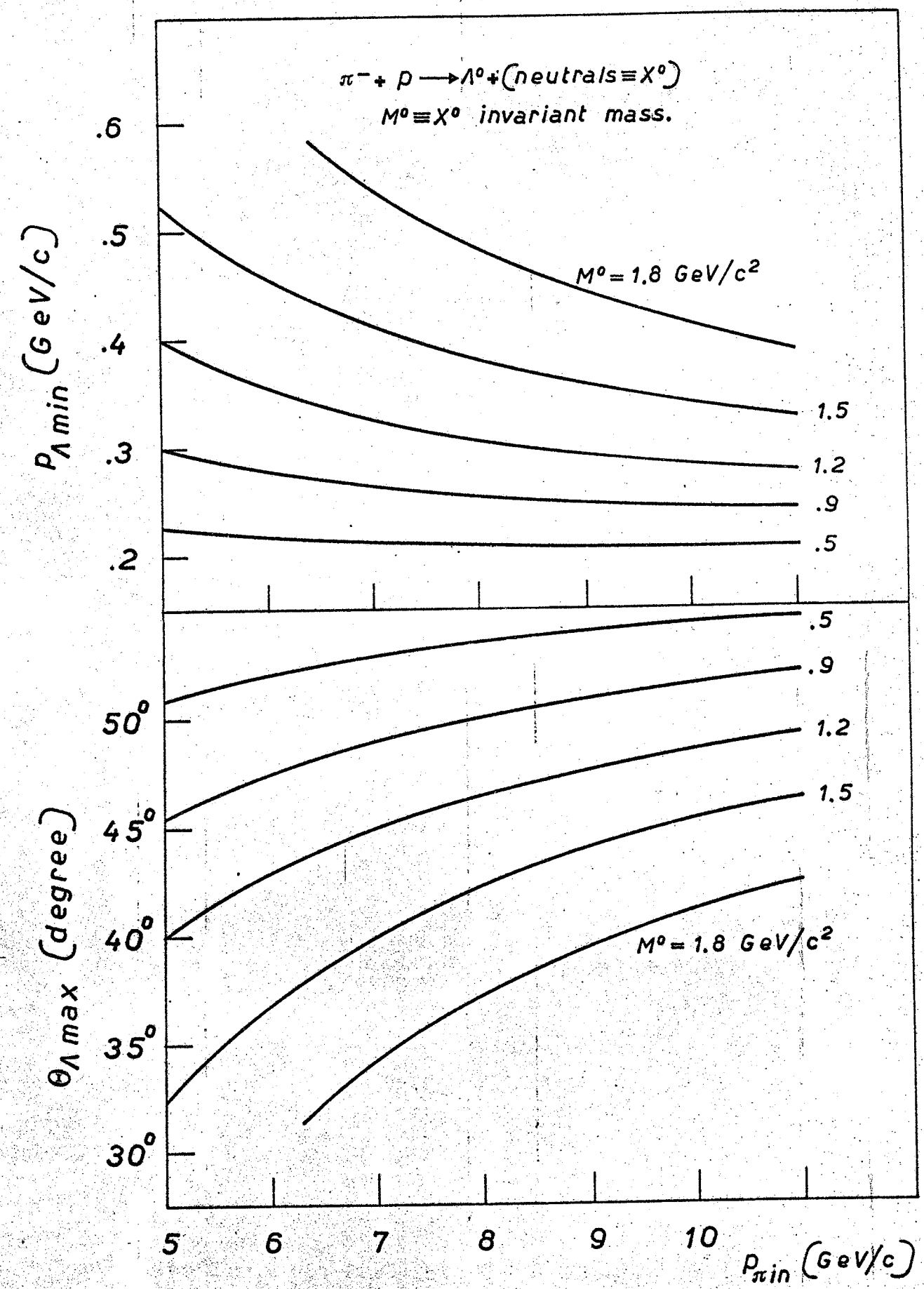
$\pi^- + p \longrightarrow \Lambda^0 + (\text{neutrals} \equiv X^0)$
$M^0 \equiv X^0$ invariant mass.
$M^0 = 1.8$ GeV/c²
1.5
1.2
.9
.5
$p_{\Lambda min}$ (GeV/c)
.6
.5
.4
.3
.2
.5
.9
1.2
1.5
$M^0 = 1.8$ GeV/c²
$\theta_{\Lambda max}$ (degree)
50°
45°
40°
35°
30°
5
6
7
8
9
10
$p_{\pi in}$ (GeV/c)

FIG. 9

Mass region —

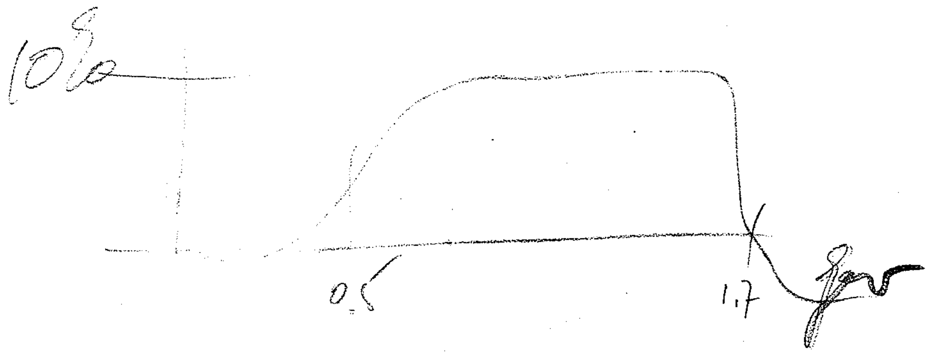

Resolution 10 to 12 MeV

tests have reached The masse of K_0 Λ K
from 0.9 GeV/c for π

tests with $3 \cdot 10^5$

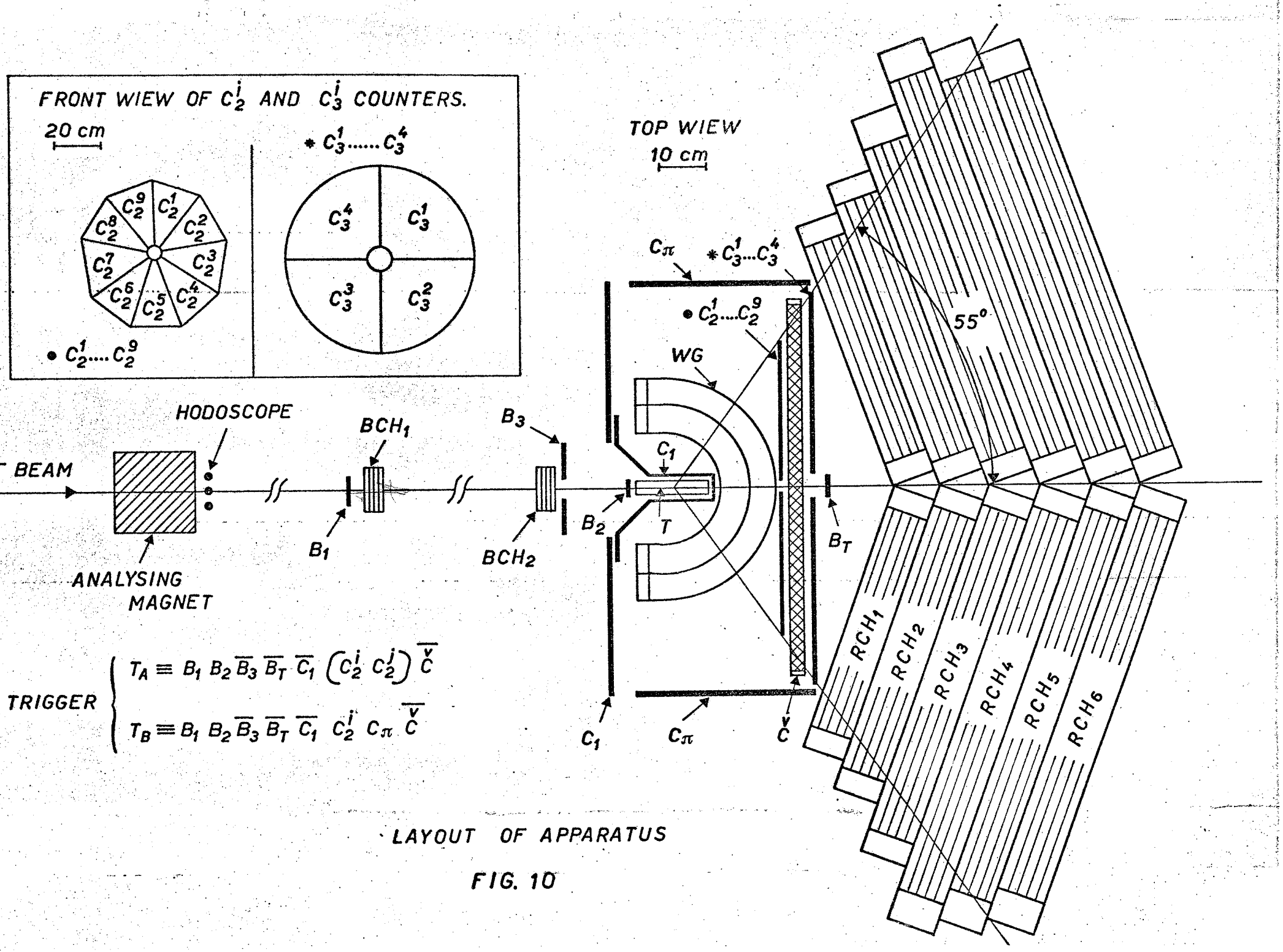

LAYOUT OF APPARATUS

FIG. 10

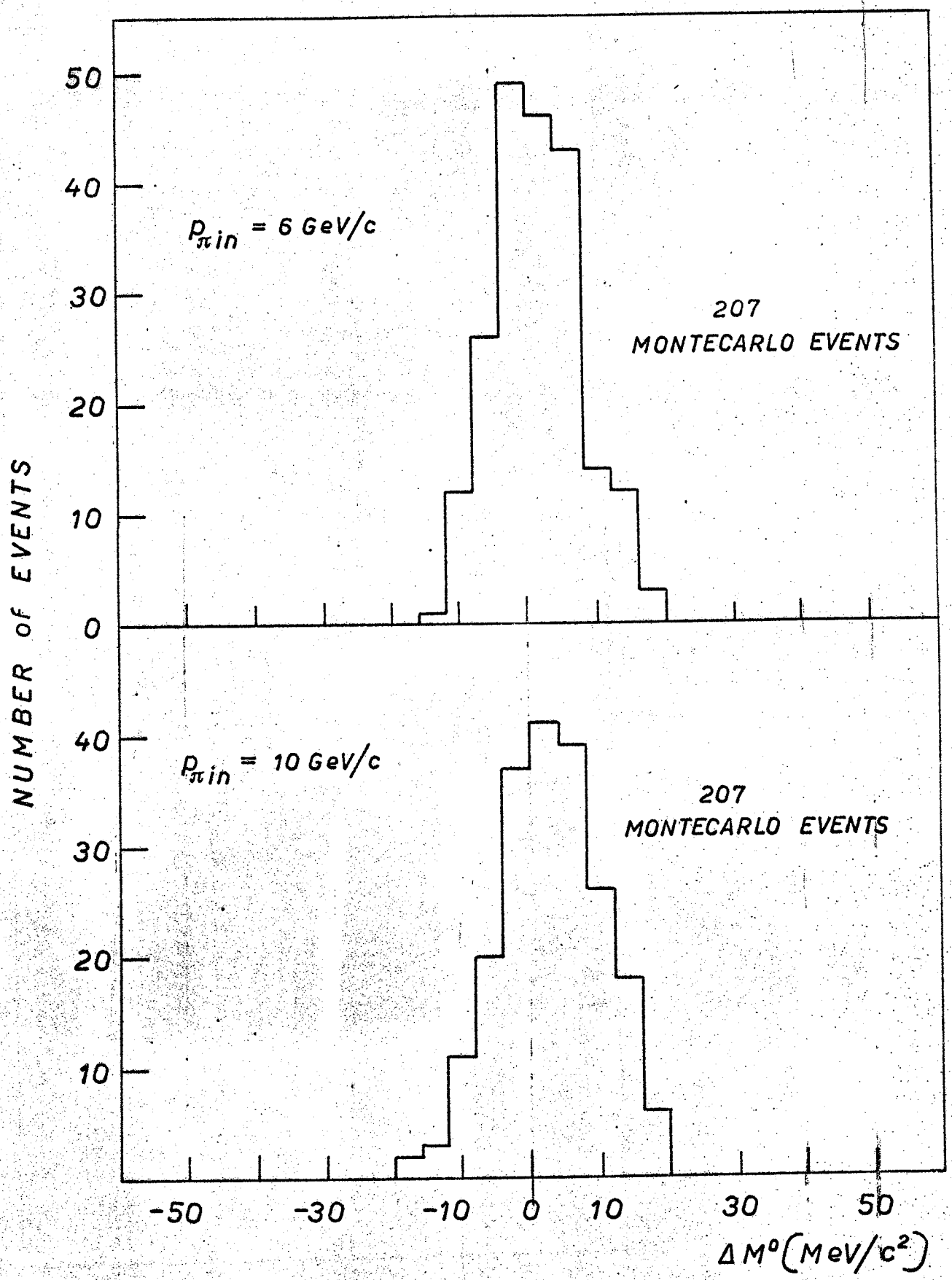
50
40
30
20
10
0
$P_{\pi in}$ = 6 GeV/c
207
MONTECARLO EVENTS
NUMBER of EVENTS
40
30
20
10
$P_{\pi in}$ = 10 GeV/c
207
MONTECARLO EVENTS
-50
-30
-10
0
10
30
50
$\Delta M^0 (MeV/c^2)$

FIG. 11

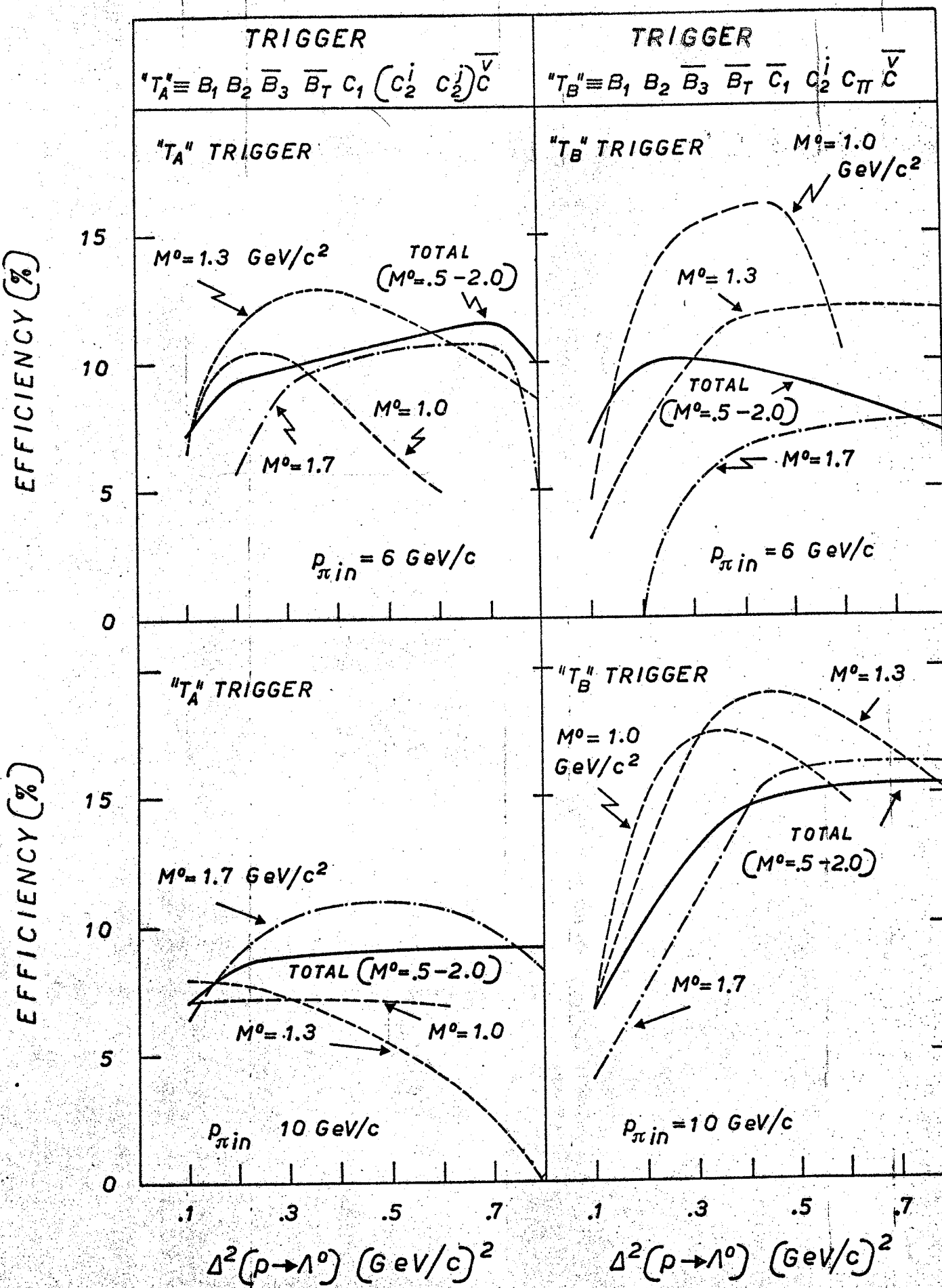
TRIGGER
"T_A" $\equiv B_1 B_2 \bar{B}_3 \bar{B}_T C_1 (C_2^i C_2^j) \bar{C}^v$
TRIGGER
"T_B" $\equiv B_1 B_2 \bar{B}_3 \bar{B}_T \bar{C}_1 C_2^i C_\pi \bar{C}^v$
"T_A" TRIGGER
"T_B" TRIGGER
M^0= 1.0 GeV/c²
M^0= 1.3 GeV/c²
TOTAL (M^0=.5 -2.0)
M^0= 1.7
$p_{\pi in}$ = 6 GeV/c
EFFICIENCY (%)
15
10
5
0
"T_A" TRIGGER
"T_B" TRIGGER
M^0= 1.7 GeV/c²
M^0= 1.3
M^0= 1.0 GeV/c²
TOTAL (M^0=.5 -2.0)
M^0= 1.0
$p_{\pi in}$ 10 GeV/c
$p_{\pi in}$ = 10 GeV/c
.1
.3
.5
.7
$\Delta^2(p \to \Lambda^0)$ (GeV/c)²

FIG. 13 b

DETECTION EFFICIENCY IF PROTON MOMENTUM ANALYSIS IS PERFORMED WITH THE A. E. G. MAGNET (GAP DIMENSIONS : 50 x 50 x 50 cm^3)

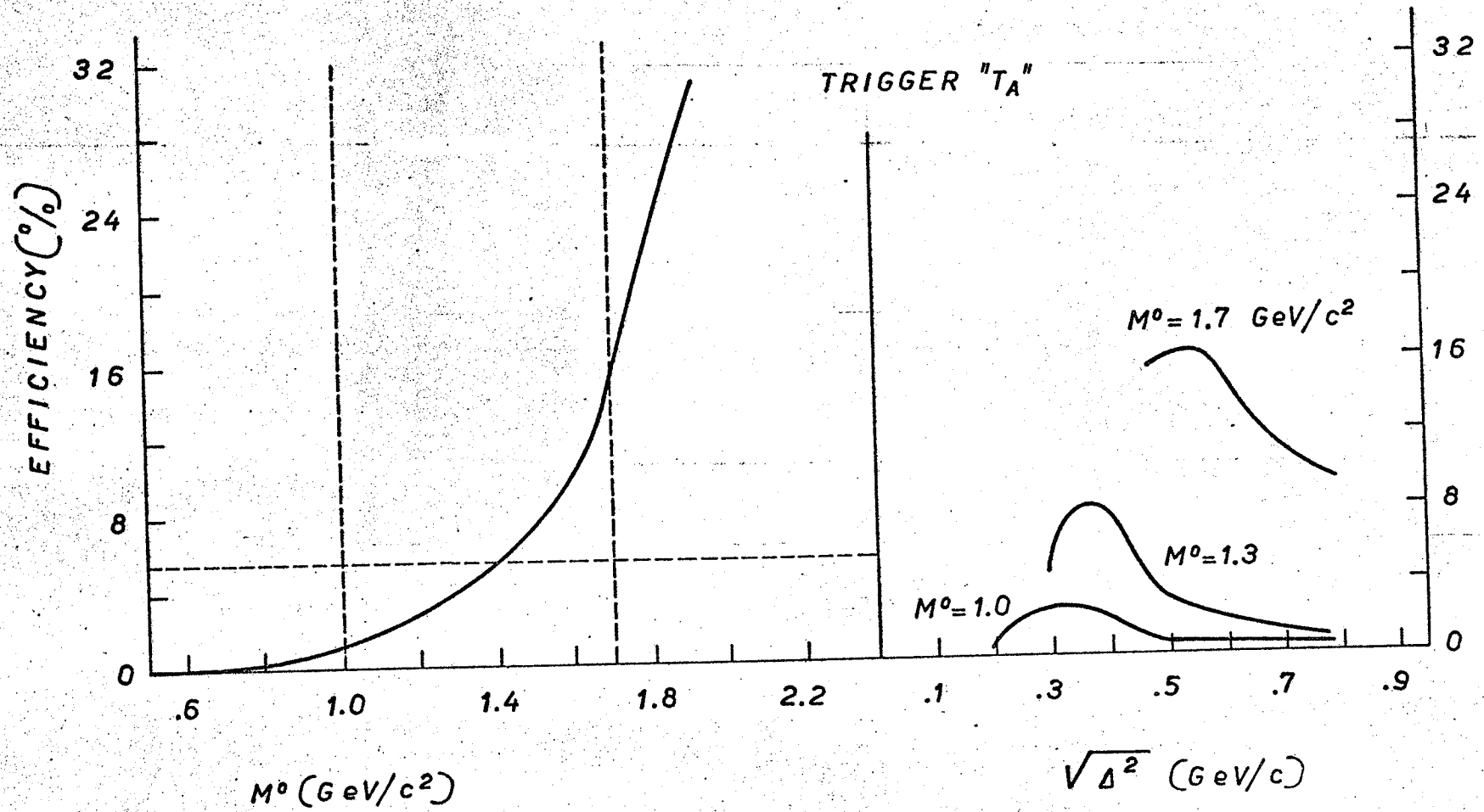

FIG. 14